

B.F. Tomandl
T. Hammen
E. Klotz
H. Ditt
B. Stemper
M. Lell

Bone-Subtraction CT Angiography for the Evaluation of Intracranial Aneurysms

PURPOSE: CT angiography (CTA) has been established for detection and therapy planning of intracranial aneurysms. The analysis of aneurysms at the level of the skull base, however, remains difficult because bone prevents a free view. We report initial clinical results of an approach for automatic bone elimination from CTA data.

MATERIAL AND METHODS: Before the bone-removal process 2 datasets are acquired: nonenhanced spiral CT with reduced dose and contrast-enhanced CTA. The software automatically registers the nonenhanced data onto the CTA data and selectively removes bone. Vascular structures, as well as brain tissue, remain visible. In this study, we investigated 27 patients with 29 aneurysms, 13 of which were located at the skull base. 3D volume-rendered images with and without bone removal were reviewed and compared with digital subtraction angiography by 2 radiologists in consensus.

RESULTS: All supraclinoid aneurysms were detected on 3D volume-rendered images of both CTA and bone-subtraction CT angiography (BSCTA). Four intracavernous and 3 paraclinoid aneurysms of the internal carotid artery were not visible or were only partially visible on conventional 3D CTA, whereas they could be optimally visualized with BSCTA. Bone removal was successful in all patients; the average additional time for postprocessing was 6.2 minutes. In 7 patients (26%), perfect bone removal without any artifacts was achieved. In most patients, some bone remnants were still present, though it did not disturb the 3D visualization of vascular structures.

CONCLUSION: BSCTA allows robust and fast selective elimination of bony structures, thus ascertaining a better analysis of arteries at the level of the skull base. This is useful for both detection and therapy planning of intracranial aneurysms.

CT angiography (CTA) becomes more and more important as the first diagnostic tool for the detection of intracranial aneurysms after acute subarachnoid hemorrhage.¹⁻⁴

The detection rate of supraclinoid aneurysms by using CTA is close to the one of digital subtraction angiography (DSA) in most recent studies performed by experienced centers with state-of-the-art equipment.³⁻⁵ Nevertheless, it is still difficult to see clearly and analyze aneurysms at the level of the skull base.⁶ Initial attempts to subtract nonenhanced from enhanced CT data, thus leading to “digital subtraction” CTA, were based on a section-by-section subtraction.⁷ This method was limited by the fact that even minor movements by patients led to insufficient subtraction and image quality. Initial results published by Venema et al with selective bone removal by using “matched mask bone elimination” were very promising.⁸ Our aim was to develop and evaluate a fast and reliable method that selectively eliminates bony structures while vascular and soft-tissue structures (brain) should still be available for analysis. In this article, we report the initial clinical results of this method in selected patients with intracranial aneurysms.

Materials and Methods

Twenty-seven patients with 29 angiographically confirmed aneurysms were investigated with CTA for therapy planning by means of 3D visualization.

Received December 25, 2004; accepted after revision May 27, 2005.

From the Division of Neuroradiology (B.F.T.), the Departments of Neurology (T.H., B.S.), and the Institute of Diagnostic Radiology (M.L.), University of Erlangen-Nuremberg, Erlangen, Germany; and Siemens Medical Solutions (E.K., H.D.), Erlangen, Germany.

B.F.T. and T.H. contributed equally to this study.

Address correspondence to: Prof. Dr. Bernd F. Tomandl, Division of Neuroradiology, Department of Neurosurgery, University of Erlangen-Nuremberg, Schwabachanlage 6, D-91054 Erlangen, Germany.

There were 6 aneurysms of the anterior communicating artery, 6 of the middle cerebral artery, 2 aneurysms of the basilar tip, and 2 aneurysms of the distal internal carotid artery (ICA). There were 4 aneurysms of the intracavernous and 9 of the paraclinoid part of the ICA, most of them arising near the origin of the posterior communicating artery. DSA of the intracranial vasculature was available in all patients by using a biplanar system (Neurostar Top, Siemens Medical Solutions, Erlangen, Germany). In one patient, 3D DSA was performed by using the same equipment. Written informed consent was obtained from all patients or their legal representatives, and the study was conducted according to the guidelines of the institutional review board. Before the CTA protocol that we regularly use in clinical routine work, we added a low-dose nonenhanced spiral CT (NECT) scan to enable the bone-removal process. The scan range included cervical body one up to the vertex. CT examinations were performed with a 4-row spiral CT scanner (Somatom Volume Zoom, Siemens Medical Solutions) with the following parameters: 4×1 mm detector collimation; table feed 3.5 mm/rotation; 120 kV; 50 mAs (nonenhanced CT); 180 mAs (contrast-enhanced CT); reconstructed section width, 1.25 mm; reconstruction increment, 0.5 mm. One hundred milliliters of nonionic iodinated contrast medium (Ultravist 300; Schering, Berlin, Germany) were injected with a power injector at a rate of 4 mL/s, and the scan delay was individually adapted by using a bolus-tracking technique.

The data were transferred to a workstation (Leonardo, Siemens Medical Solutions) equipped with a prototype software tool for bone subtraction developed by Siemens Medical Solutions. The subtraction process is started by loading both the nonenhanced and the contrast-enhanced data in memory. When shape and CT value distribution of bony structures in both datasets are used, the software automatically matches the volumes by using a rigid transformation model.⁹ The software then starts the automatic bone removal process that selectively eliminates only bone, thus retaining both soft tissue

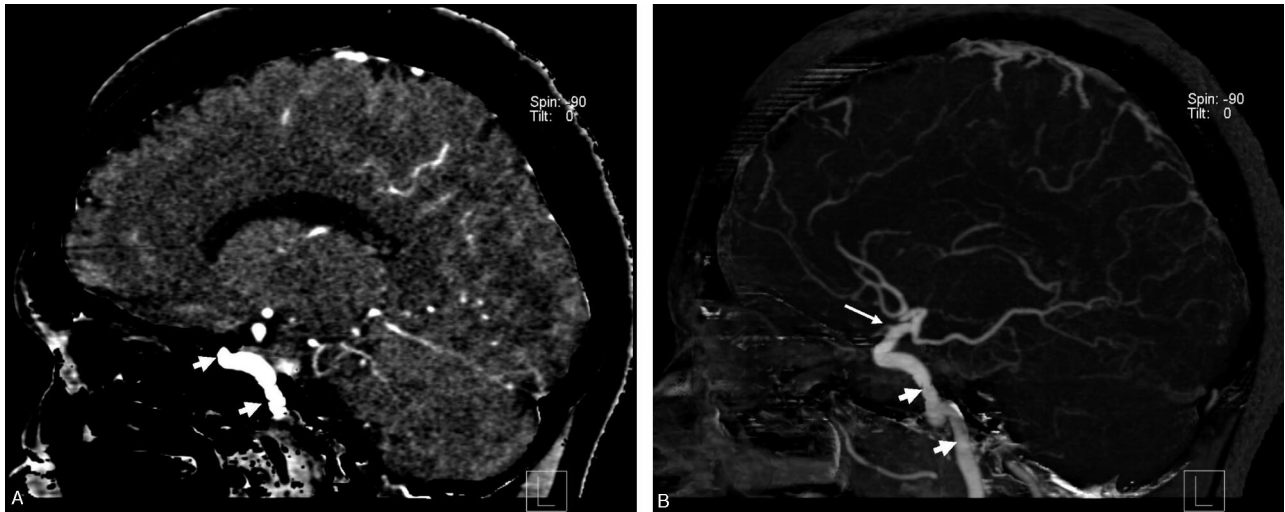


Fig 1. Illustration of the bone-removal process.

A, Sagittal multiplanar reformation of the data after bone removal shows the contrast-enhanced vascular structures (*arrows*) as well as brain tissue.

B, Sagittal maximum intensity projection image (15-mm thickness) demonstrates the intraosseous parts of the internal carotid artery (*short arrow*) as well as the origin of the ophthalmic artery (*long arrow*).

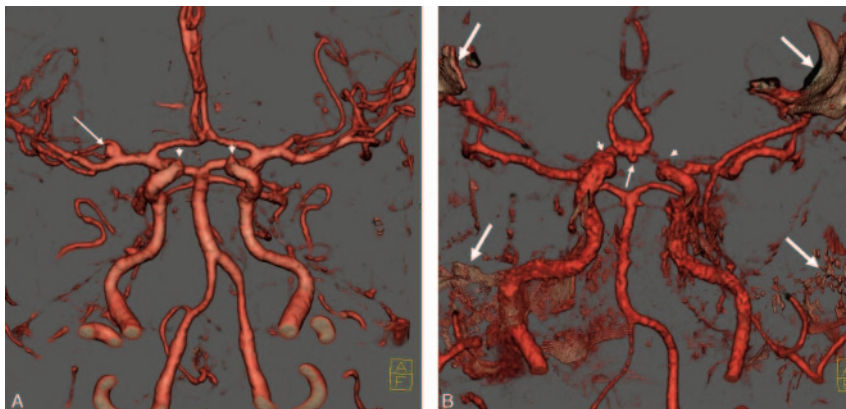


Fig 2. Different qualities of bone removal, anterior-inferior view. Note the visibility of the origin of the ophthalmic artery in both images (*arrowheads*).

A, “Excellent” bone removal without artifacts. There is a small aneurysm of the right middle cerebral artery (*arrow*).

B, “Moderate” result with remnants of bone (*arrows*) because of movement of the patient during one of the scans. The arteries within the skull base are still visible. There is a small aneurysm of the anterior communicating artery (*arrow*).

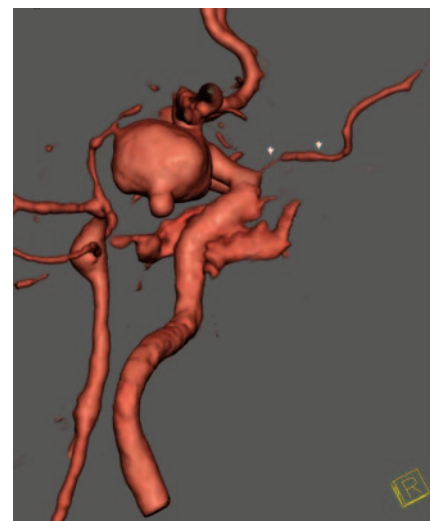


Fig 3. Optimal visualization of the ophthalmic artery (*arrowheads*) of the right ICA in this patient with a large aneurysm of the ICA from a lateral view.

(eg, brain) and contrast-filled arteries and veins (Fig 1). This process is similar to the “match mask bone elimination” as described by Venema et al.⁸ We refined the determination of the contrast bone borders, however, by only initially using a global threshold for the segmentation of bony structures in the nonenhanced CT images. The threshold is then locally adapted if vessels are in the vicinity to avoid creating artificial stenoses. The resulting bone structures are selectively eliminated from the contrast-enhanced data. Thus, “subtraction” of brain tissue is avoided so that all soft tissue structures are still available for further evaluation in the resulting volume. The resulting data were used for 3D visualization by using direct volume rendering. Two experienced (neuro-) radiologists (B.F.T., M.L.) reviewed the 3D models concerning image quality as measured by quality of subtraction, visibility of the intracavernous part of the ICA, and visibility of the ophthalmic arteries.

Quality of the subtraction process. The quality of the resulting subtracted volume data were rated “excellent” when only vascular structures were visible without any artifacts such as residual bone

(Fig 2A). A “good” result was assumed when some bone remnants were visible without disturbing a free view of the vascular structures. A result was rated “moderate” when large bone remnants remained or parts of the arteries were affected by the subtraction process (Fig 2B).

Visibility of the ophthalmic arteries. An “excellent” depiction was defined as a visualization of the ophthalmic artery from the origin of the ICA to the intraorbital portion (Fig 3). A “moderate” result meant that only parts or at least the origin of the ophthalmic arteries were visible (Fig 2). If not even the origin of an ophthalmic artery was visible, the result was rated as “insufficient.”

Visibility of the intracavernous ICA on volume-rendered images. An image was rated “excellent” when the cavernous sinus was not visible at all (Fig 4A). A “good” result was assumed when the visible parts of the cavernous sinus did not disturb the evaluation of the intracavernous part of the ICA. If the cavernous sinus was enhanced so that parts of the ICA were not visible, the result was rated “moderate.” In these cases, it was necessary to use multiplanar refor-



Fig 4. Prominent cavernous sinus (arrowheads).

A, 3D volume-rendered image with high opacity and shading does not allow evaluation of the intracavernous part of the left ICA completely on this medial view.

B, Transparent (low-opacity) volume-rendered image allows for a good evaluation of the intracavernous portion of the ICA (arrow).

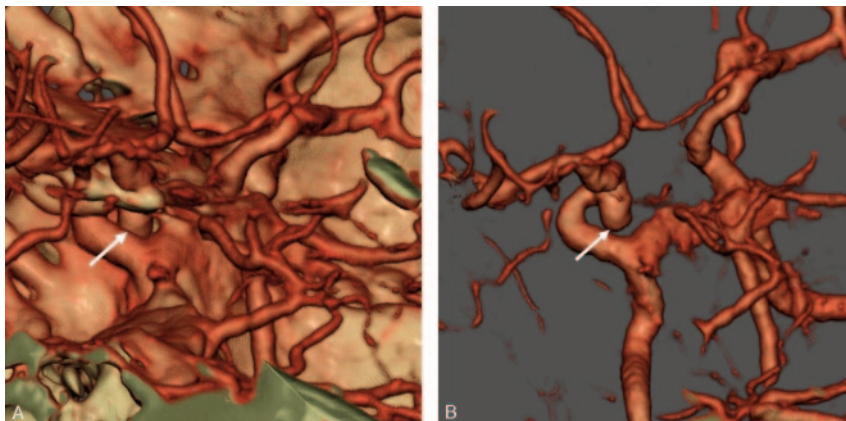


Fig 5. Aneurysm of the left infraclinoid ICA, left-superior view.

A, On standard CT angiography the aneurysm is hardly visible (arrow) due to obscuration by the anterior clinoid process.

B, Bone-subtraction CT angiography (BSCTA) clearly shows the complete shape of the aneurysm (arrow).

mation, maximum intensity projection (MIP), or transparent (low-opacity) volume rendering for exact evaluation of this area (Fig 4B).

In a second session, the nonsubtracted CTA images were evaluated by using the same volume rendering technique preset for the detection and delineation of aneurysms. Afterward, the investigators directly compared subtracted and unsubtracted images by using identical views and settings for volume rendering interactively on the workstation in consensus. If parts of the parent vessel or the aneurysm were not visible because of overlying structures or partial volume effects on the unsubtracted images though these details were clearly seen on subtracted images, bone-subtraction CT angiography (BSCTA) was rated superior. DSA served as the standard of reference, and for this part of the evaluation both investigators were aware of the results from DSA.

Results

The mean additional postprocessing time needed for the bone-removal process was 6.2 minutes. This did not include the time for data transfer from the CT scanner to the workstation, which is about 3–4 minutes, depending on the number of source images.

The quality of the resulting volume data were rated “excellent” in 7 (26%) of the patients (Fig 2A) and “good” in 18 (67%) of the patients. In 2 cases only “moderate” results were seen (7%). In these, severe artifacts of incomplete bone removal remained, caused by movement of the patient during acquisition of one or both scans. This was verified by reviewing the data with interactive multiplanar reformation, where the offset of contiguous sections was clearly visible. The interpre-

tation of intracranial arteries, including those in the area of the skull base was still possible, however, in both cases (Fig 2B).

Excellent visualization of both ophthalmic arteries was seen in 6 patients (22%). In 4 patients (15%), only one ophthalmic artery was visible (Fig 3). In the remaining 17 patients (63%), only a

moderate visualization of both ophthalmic arteries was possible (Fig 2).

The cavernous sinus was not visible, thus giving a free view to the ICA in 7 cases (26%), so these images were rated “excellent” (Fig 4A). In 18 cases, the visualization of the intracavernous ICA was “good.” In 2 cases (7%), “moderate” results were seen. In these cases, it was necessary to use multiplanar reformation, MIP, or transparent (low-opacity) volume rendering for exact evaluation of this area (Fig 4B).

Comparing CTA and BSCTA, all aneurysms located above the anterior clinoid process were sufficiently demonstrated with both methods. Of the 13 aneurysms located at the ICA, 4 intracavernous aneurysms were not and 3 paraclinoid aneurysms were only partially visible on CTA, whereas all aneurysms were seen completely (including parent vessel, neck, and dome) on BSCTA (Fig 5). Thus, 7 of 13 aneurysms (54%) located at the ICA were better visible with BSCTA.

In one patient with a large aneurysm of the ICA at the origin of the posterior communicating artery, 3D DSA was also available. The information obtained by both studies was similar (Fig 6).

Discussion

DSA is still the most sensitive tool for the detection of intracranial aneurysms and other vascular malformations. CTA is increasingly applied for detection and therapy planning of intracranial aneurysms. The reported sensitivity of CTA is in the range of 70%–96% depending on the size and location of an aneurysm.^{3,4,6,10,11}

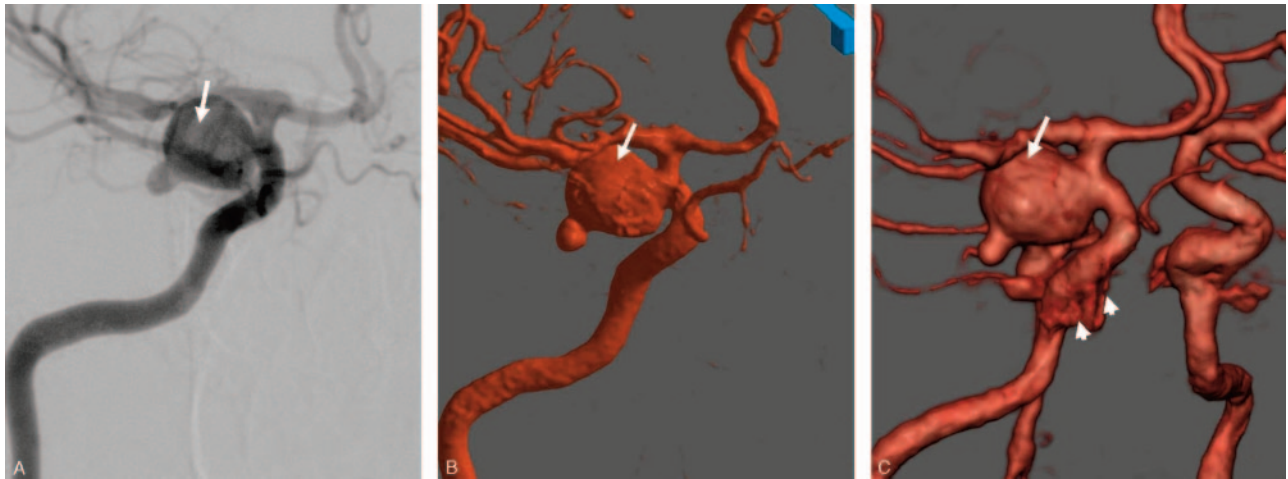


Fig 6. Comparison of digital subtraction angiography (DSA), 3D DSA and BSCTA. Patient with a large aneurysm of the right ICA (arrows), right anterior oblique view. A, DSA. B, 3D DSA, direct volume rendering. C, BSCTA. The cavernous sinus does not disturb the interpretation of the image (arrowheads).

In most of these studies, 3D visualizations of the intracranial vessels were used to assess the value of CTA. The section images were then transferred to a workstation, and 3D visualization of the vascular structures performed. The aim of 3D visualization is to extract the information of vascular structures from the volume. Regardless of the applied algorithm, these methods always lead to reduction of information. Therefore, it is mandatory to review the source images before performing 3D visualization. Although numerous studies with improved image acquisition (multisection CT) and postprocessing (direct volume rendering) have been published, CTA has still not been able to replace DSA as the gold standard for the detection of intracranial aneurysms. One reason may be that CTA is not a uniformly standardized method, particularly with regard to image postprocessing.¹² In a study performed at our institution, we used high-resolution direct volume rendering for the detection of aneurysms from CTA data in 87 patients with 109 aneurysms. The most important finding of this study was that 57% of false-negative findings were related to aneurysms located near to or within the skull base, though they contributed to only 36% of all aneurysms.¹³

This shows the necessity to develop a stable method for the elimination of bone to increase the sensitivity of CTA.

Several solutions for this problem have been advocated. Manual elimination of bone is very time consuming and user dependent and thus is not applicable to routine clinical work.¹⁰ The idea of subtracting nonenhanced from contrast-enhanced CT studies was first published by Gorzer in 1994.⁷ The subtraction process was based on a section by section approach and was therefore very susceptible to patient motion.¹⁴ Another approach is based on the detection of connected voxels with the use of seeding points.¹⁵ Because the skull base is very inhomogeneous concerning its attenuation, a threshold-based approach is not reliable. In addition, the seeds have to be placed by a user, thus leading to an undesirable user dependence of the result. A method that is close to our approach has been proposed by Venema et al.⁸ Here the bone was selectively removed with an approach the authors called “matched mask bone elimination.” They showed that registra-

tion and “matching” of nonenhanced and contrast-enhanced data provides significantly better results than simple subtraction of each section. The time for postprocessing of their study was about 1 hour and was reduced to 15 minutes in another recently published study of the same working group.¹⁶ In our study, the average time for postprocessing was only 6.2 minutes. This seems to be acceptable in routine clinical work, especially because no user interaction is required.

Recently Vega-Higuera et al proposed a novel threshold-based approach for the elimination of the skull base by using what they called “bidimensional transfer functions” for direct volume visualization of aneurysms involving the skull base.¹⁷ In this approach, not only are voxel intensities considered, but gradient magnitudes are also extracted from the data to create the mapping from volume data to colors and opacities. Transfer functions can be created interactively, and effective osseous tissue removal is obtained even if vessels are embedded. The obtained results are promising and if the clinical value of this approach can be proved the acquisition of a nonenhanced dataset will no longer be necessary.

Our study also showed that matching of the volume data is not disturbed by patient movement *between* the 2 studies. Movement *during* one or both studies was present in 2 of our patients, corrupting the consistency of the dataset and leading to considerable artifacts (Fig 2B). With the introduction of new scanners acquiring 64 sections per rotation, this problem will become less severe, because the base of the skull can be covered in <2 seconds. Careful patient instruction is helpful and the use of special restraining devices might completely avoid patient movement.¹⁸

An important finding is that at least the origin of the ophthalmic arteries was visible in all studies. This allows clear differentiation between paraclinoid and cavernous sinus aneurysms, which is important for planning therapy of a detected aneurysm.¹⁹ Bone removal is especially useful for therapy planning in aneurysms involving the intracavernous and supraophthalmic part of the ICA as demonstrated in Fig 7.

The main disadvantage of BSCTA is the increased radiation dose due to the second scan. This seems to be acceptable when

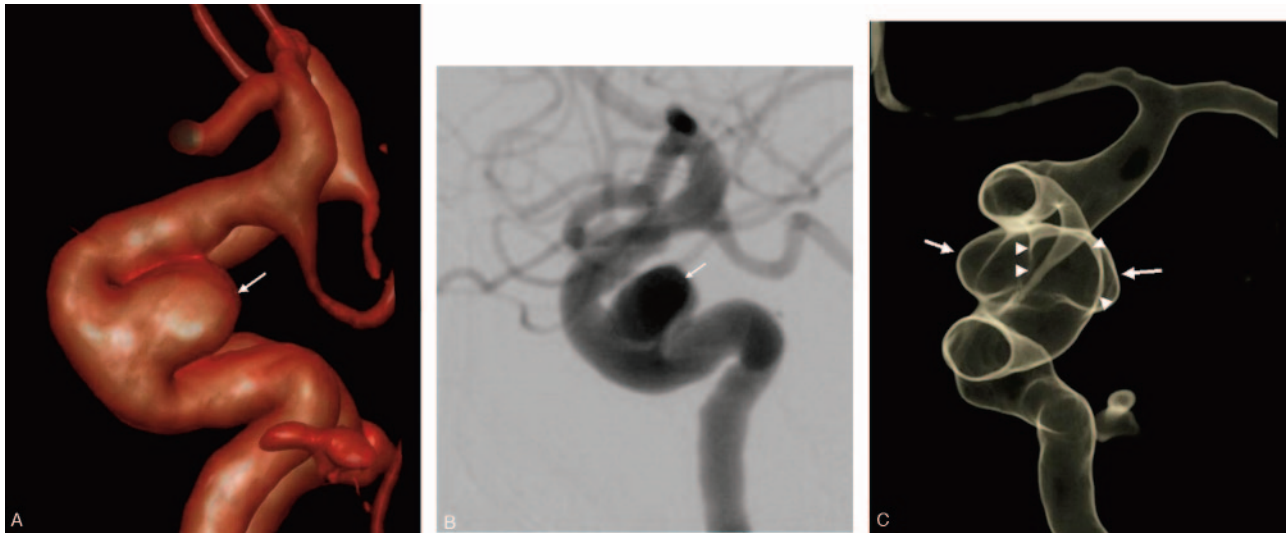


Fig 7. Use of BSCTA for therapy planning of an intracavernous aneurysm of the left ICA (arrows).

A, BSCTA, lateral view of the left ICA.

B, DSA, lateral view of the left ICA.

C, Transparent (low-opacity) volume rendering allows visualization of the borders of the aneurysm's broad neck (arrowheads) from an anterior view, which is useful for therapy planning. This aneurysm was finally treated by means of stent-protected coiling.

low-dose settings are chosen for the nonenhanced scan. As used by us and by other study groups, an effective increase of exposure by 20%–25% above the level of standard CTA seems to be sufficient to implement subtraction techniques.^{8,18} Such a relatively small increase of exposure is well within the variance of exposure values for standard CTA in various studies on different CT scanners. For our scanner, the effective dose for the original CTA data is between 1.0 (only base of skull and circle of Willis) and 2.0 mSv (whole intracerebral vasculature). If the NECT scan is restricted to the skull base the additional effective dose amounts to 0.25 mSv. If noncontrast spiral CT is used as the standard examination of patients with suspected subarachnoid hemorrhage instead of incremental CT, this scan can readily be used for the subtraction process.²⁰

Conclusion

BSCTA is a fast and stable method that improves the detection and interpretation of aneurysms near to the skull base that is easy to use and thus applicable in routine clinical work. It is clearly an important step toward the standardization of CTA, which is a mandatory precondition to replace DSA as a gold standard for the detection of intracranial aneurysms.

References

1. Kouskouras C, Charitanti A, Giavroglou C, et al. Intracranial aneurysms: evaluation using CTA and MRA: correlation with DSA and intraoperative findings. *Neuroradiology* 2004;46:842–50
2. Hoh BL, Cheung AC, Rabinov JD, et al. Results of a prospective protocol of computed tomographic angiography in place of catheter angiography as the only diagnostic and pretreatment planning study for cerebral aneurysms by a combined neurovascular team. *Neurosurgery* 2004;54:1329–40; discussion 1340–42
3. Karamessini MT, Kagadis GC, Petsas T, et al. CT angiography with three-dimensional techniques for the early diagnosis of intracranial aneurysms: comparison with intra-arterial DSA and the surgical findings. *Eur J Radiol* 2004;49:212–23
4. Teksam M, McKinney A, Casey S, et al. Multi-section CT angiography for detection of cerebral aneurysms. *AJNR Am J Neuroradiol* 2004;25:1485–92
5. Tipper G, U-King-Im JM, Price SJ, et al. Detection and evaluation of intracranial aneurysms with 16-row multislice CT angiography. *Clin Radiol* 2005;60:565–72
6. White PM, Wardlaw JM, Easton V. Can noninvasive imaging accurately depict intracranial aneurysms? A systematic review. *Radiology* 2000;217:361–70
7. Gorzer H, Heimberger K, Schindler E. Spiral CT angiography with digital subtraction of extra- and intracranial vessels. *J Comput Assist Tomogr* 1994;18:839–41
8. Venema HW, Hulsmans FJ, den Heeten GJ. CT angiography of the circle of Willis and intracranial internal carotid arteries: maximum intensity projection with matched mask bone elimination-feasibility study. *Radiology* 2001; 218:893–98
9. Pluim JP, Maintz JB, Viergever MA. Mutual-information-based registration of medical images: a survey. *IEEE Trans Med Imaging* 2003;22:986–1004
10. Schwartz RB, Tice HM, Hooten SM, et al. Evaluation of cerebral aneurysms with helical CT: correlation with conventional angiography and MR angiography. *Radiology* 1994;192:717–22
11. Liang EY, Chan M, Hsiang JH, et al. Detection and assessment of intracranial aneurysms: value of CT angiography with shaded-surface display. *AJR Am J Roentgenol* 1995;165:1497–502
12. Tomandl BF, Kostner NC, Schempershofe M, et al. CT angiography of intracranial aneurysms: a focus on postprocessing. *Radiographics* 2004;24:637–55
13. Tomandl B, Schempershofe M, Koestner N, et al. 3D CT-angiography for the detection of intracranial aneurysms: what are the reasons for false-negative and false-positive findings? *Radiology* 2003;suppl:319
14. Imakita S, Onishi Y, Hashimoto T, et al. Subtraction CT angiography with controlled-orbit helical scanning for detection of intracranial aneurysms. *AJNR Am J Neuroradiol* 1998;19:291–95
15. Abrahams JM, Saha PK, Hurst RW, et al. Three-dimensional bone-free rendering of the cerebral circulation by use of computed tomographic angiography and fuzzy connectedness. *Neurosurgery* 2002;51:264–68; discussion 268–69
16. Majoie CB, van Straten M, Venema HW, et al. Multisection CT venography of the dural sinuses and cerebral veins by using matched mask bone elimination. *AJNR Am J Neuroradiol* 2004;25:787–91
17. Vega-Higuera F, Sauber N, Tomandl BF, et al. Enhanced 3D-visualization of intracranial aneurysms involving the skull base. In: Ellis RE, Peters TM, eds. *Proceedings of medical image computing and computer assisted intervention*. Montreal: Springer-Verlag;2003:256–63
18. Jayakrishnan VK, White PM, Aitken D, et al. Subtraction helical CT angiography of intra- and extracranial vessels: technical considerations and preliminary experience. *AJNR Am J Neuroradiol* 2003;24:451–55
19. Gonzalez LF, Walker MT, Zabramski JM, et al. Distinction between paraclinoid and cavernous sinus aneurysms with computed tomographic angiography. *Neurosurgery* 2003;52:1131–37; discussion 1138–39
20. Kuntz R, Skalej M, Stefanou A. Image quality of spiral CT versus conventional CT in routine brain imaging. *Eur J Radiol* 1998;26:235–40